Transition Met Chem
DOI 10.1007/s11243-014-9819-8

Understanding the electronic and π-conjugation roles of quinoline on ligand substitution reactions of platinum(II) complexes

Grace Kinunda · Deogratius Jaganyi

Received: 14 February 2014 / Accepted: 12 March 2014

Abstract A kinetic and mechanistic study of chloride substitution by thiourea nucleophiles, namely thiourea, *N*-methylthiourea, *N*,*N*-dimethylthiourea and *N*,*N*,*N*′,*N*′-tetramethylthiourea in the complexes chlorobis-(2-pyridylmethyl) amineplatinum(II) (Pt1), chloro *N*-(2-pyridinylmethyl)-8-quinolinamineplatinum(II) (Pt2), chloro *N*-(2-pyridinylmethylene)-8-quinolinamineplatinum(II) (Pt3) and chlorobis(8-quinolinyl)amineplatinum(II) (Pt4) was undertaken under *pseudo*-first-order conditions using UV–visible spectrophotometry. The study showed that lability of the chloro leaving group is dependent on the strength of π-interactions between the filled *d*π-orbitals of the metal and the empty π*-orbitals of the chelating ligand in the following manner: Pt1 > Pt3 > Pt2 > Pt4. Introduction of the quinoline moiety within the non-labile chelated framework of the Pt(II) complexes results in a more electron-rich metal centre which retards the approach of the nucleophile through repulsion. Moreover, the net σ-effect of the ligand moiety plays a significant role in controlling the reactivity of the complexes. The experimental results are interpreted with the aid of computational data obtained by density functional theory (B3LYP(CPCM)/LANL2DZp//B3LYP/-LANL2DZp) calculations. The mode of substitution remains associative as supported by negative entropies and the dependence of the second-order rate constants on the concentration of entering nucleophiles.

Electronic supplementary material The online version of this article (doi:10.1007/s11243-014-9819-8) contains supplementary material, which is available to authorized users.

G. Kinunda · D. Jaganyi (✉)
School of Chemistry and Physics, University of KwaZulu-Natal, Scottsville 3209, South Africa
e-mail: jaganyi@ukzn.ac.za

Introduction

The rate of substitution of square planar Pt(II) tridentate chelates of the type $[Pt(NNN)X]^+$ where X = chloride or aqua ligand can be varied by tuning structural, steric and electronic properties of the non-labile ligands [1, 2]. Most previous studies have involved monofunctional tridentate Pt(II) complexes, $[Pt(dien)Cl]^+$, [3–5] $[Pt(bpma)Cl]^+$ [1, 2], $[Pt(terpy)Cl]^+$, [6–18] and $[Pt(tpdm)Cl]^+$, [19, 20] (where dien = diethylenetriamine, bpma = bis-(2-pyridylmethyl)amine, terpy = 2,2′:6′,2″-terpyridine and tpdm = terpyridinedimathane). These complexes are highly stable even under acidic conditions due to the chelate effect and synergistic combination of σ-donor and π-acceptor *N*-heterocyclics that incorporate five-membered rings [21].

van Eldik and co-workers [6–11, 22–24] have reported that the reactivity of Pt(terpy), Pt(bpma) and Pt(dien) increased in the order of Pt(terpy) > > Pt(bpma) > Pt(dien) due to the introduction of π-backbonding by systematically substituting amine ligands with pyridine donor groups. The higher reactivity of approximately 3–5 orders of magnitude reported for Pt(terpy) compared to Pt(bpma) and Pt(dien) was attributed to effective communication through π-backbonding of the in-plane pyridine moieties in the terpy ligand. This was shown to increase the electrophilicity of the metal centre and stabilize the five-coordinate transition state relative to the ground state during an associative substitution process. In a related study, it was found that *cis*-π backbonding is stronger than *trans*-π backbonding [25]. On the other hand, *cis*-σ-donor effects have been reported to slow down the lability of the leaving group in Pt(II) complexes [1, 2, 21, 25] through the accumulation of electron density on the Pt centre, while the *trans*-σ-donor effect accelerates

Published online: 25 March 2014

the rate of substitution reactions by the well-known *trans*-labilization effect [26]. In recent studies by our group, it was shown that if one of the outer pyridine rings in the terpy system is substituted by an isoquinoline ligand in the *cis* position, a net *cis*-σ-donor effect is experienced by the complex, decreasing the lability of the leaving group [27]. When the pyridine group is replaced by a pyrazine moiety, the lability of the leaving group is enhanced due to stronger π-acceptor properties of pyrazine as a ligand [28]. Thus, in principle, such tuning of the lability of the leaving group in Pt(II) complexes plays an important role in the development of new antitumour agents. This is evident by the number of platinum-based complexes that have been synthesized and investigated for their anticancer efficacy since the discovery of [*cis*-diamminedichloroplatinum(II)], (cisplatin) in 1969 [29], which is greatly hampered by severe side effects and drug resistance [30–33].

To extend our understanding of the role played by σ-donation of the quinoline moiety and the π-conjugation system on ligand substitution reactions in tridentate monofunctional Pt(II) complexes, a series of ligands with quinoline ring systems coordinated to Pt(II) via amine/imine bonds was undertaken. Based on data available in the literature, the expectation was that by increasing the electronic communication through π-conjugation the reactivity of the Pt(II) centre towards substitution would be enhanced, but this will be in competition with quinoline's σ-donation. Therefore, Pt(II) compounds, chlorobis-(2-pyridylmethyl)amineplatinum(II), (Pt1), chloro *N*-(2-pyridinylmethyl)-8-quinolinamineplatinum(II), (Pt2), chloro *N*-(2-pyridinylmethylene)-8-quinolinamineplatinum(II), (Pt3) and chlorobis(8-quinolinyl)amineplatinum(II), (Pt4) were synthesized and their kinetics investigated using sulphur donor nucleophiles; thiourea (TU), 1-methylthiourea (MTU), 1,3-dimethyl-2-thiourea (DMTU) and 1,1,3,3,-tetramethyl-2-thiourea (TMTU). Thiourea nucleophiles were chosen due to their good nucleophilicity, high solubility and suitability as good model compounds for thiolate and thioether groups present in the cell. The structures of the complexes studied are summarized in Scheme 1. DFT calculations were performed to provide further understanding of the experimental results.

Experimental

Materials

All synthetic work was performed under an inert atmosphere of nitrogen. Solvents used for synthesis and kinetic measurements were dried by standard methods [34] and distilled prior to use. Tris(dibenzylideneacetone)dipalladium(0) (97 %), *rac*-2,2′-bis(diphenylphosphino)-1,1′-binaphthyl (97 %), 8-bromoquinoline (98 %), 8-aminoquinoline (98 %), NaO^{t}Bu (97 %), pyridine-2-carboxyaldehyde (99 %), 2-picolylchloride hydrochloride (98 %), lithium perchlorate (98 %), sodium borohydride (98 %), 2-picolylamine, BPMA (99 %) and thiourea nucleophiles were obtained from Aldrich. Potassium tetrachloroplatinate (K_2PtCl_4 99.99 %) was obtained from Strem. All other chemicals were of analytical grade and were used as supplied.

Synthesis of the ligands

Bis(8-quinolinyl)amine (BQA): A two-necked flask was charged with tris(dibenzylideneacetone)dipalladium(0) (22 mg, 0.024 mmol), *rac*-2,2′-bis(diphenylphosphino)-1,1′-binaphthyl (29.87 mg, 0.048 mmol) and dry toluene (10 mL) under an inert atmosphere of nitrogen. The resulting solution was stirred for 5 min, and 8-bromoquinoline (0.16 mL, 1.201 mmol), 8-aminoquinoline (0.1737 g, 1.205 mmol) and additional dry toluene (20 mL) were added. The subsequent addition of NaO^{t}Bu (0.1387 g, 1.437 mmol) resulted in a red solution that was left stirring vigorously for 3 days at 110 °C. The solution was then allowed to cool and filtered through a silica plug, then extracted with dichloromethane to ensure complete removal of the desired product. Concentration of the collected extracts and removal of solvent yielded a crude red solid. Purification by flash chromatography on silica gel (4:1 toluene/ethyl acetate) yielded an orange solid as a spectroscopically pure compound. Characterization data for BQA compared favourably with that previously reported [35]. Yield: 24.7 mg, Orange solid (76 %). ^{1}H NMR ($CDCl_3$, 400 MHz,): δ/ppm = 10.64 (s, 1H), 8.92 (dd, 2H), 8.15 (dd, 2H), 7.90 (d, 2H), 7.53–7.44 (m, 4H),

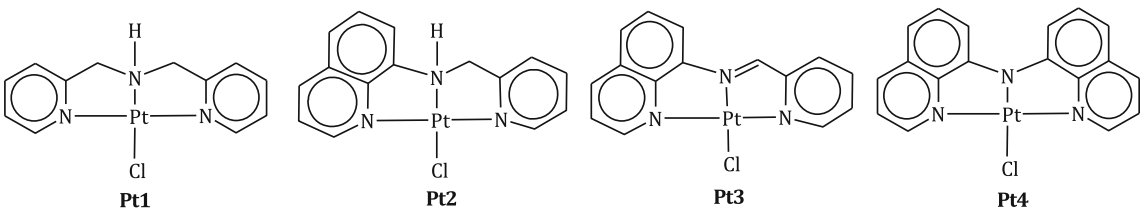

Scheme 1 Structures of investigated Pt(II) complexes (charges are omitted for clarity)

7.33 (d, 2H). ^{13}C NMR ($CDCl_3$, 400 MHz,): δ/ppm = 148.1, 140.0, 138.8, 136.2, 129.0, 127.1, 121.6, 117.9 and 110.1. *Anal. Calcd*. for $C_{18}H_{13}N_3$: C 79.70, H 4.80, N 15.50. *Found* C 79.63, H 5.01, N 15.24. TOF MS ES$^+$: *m/z*, $[M + Na]^+ = 294.10$.

N-(2-pyridinylmethyl)-8-quinolinamine, Qui-py: The published method [36] was followed with minor modifications. To a suspension of anhydrous $MgSO_4$ (20 mmol) in CH_2Cl_2 (30 mL) was added 2-pyridinecarboxaldehyde (5 mmol) followed by 8-aminoquinoline (5 mmol). After the mixture had been stirred for 3 h at room temperature, the suspension was filtered, washed with CH_2Cl_2 and the solvent removed under vacuum. The yellow oil which resulted was dissolved in 20 mL CH_3CN and cooled to −5 °C followed by addition of glacial acetic acid (0.3 mL, 5 mmol). The resulting imine compound was reduced by careful addition of a suspension of sodium borohydride (0.3783 g, 10 mmol) in absolute ethanol (10 mL) over a period of 1 h at −5 °C. A white precipitation was formed. The colour of the solution changed from yellow to red by the end of addition. After stirring for 18 h at room temperature, the reaction mixture was quenched with 5 M HCl (30 mL) and finally heated at 60 °C for 2 h until no more hydrogen was evolved. The resultant white precipitate was filtered off and the filtrate concentrated in *vacuo* and then redissolved in water (20 mL). The resulting yellow aqueous solution was basified by adding NaOH under ice-water temperature. The obtained oil was extracted with ether and dried over $MgSO_4$. Evaporation of the solvent yielded a brown oil. Yield: 686.7 mg, (63 %). ^{1}H NMR ($CDCl_3$, 400 MHz,) δ/ppm = 9.82(s,1H), 8.76(td, 1H), 8.62 (d, 1H), 8.05(ddd, 1H), 7.60 (td, 1H), 7.42–7.29 (m, 2H), 7.14 (dd, 1H), 7.09(dd, 1H), 6.92(dd, 1H), 6.61 (d, 1H), 4.47 (s, 2H). ^{13}C NMR ($CDCl_3$, 400 MHz,): δ/ppm = 159.3, 149.3, 147.6, 136.7, 136.3, 127.7, 127.4, 122.0, 121.4, 121.3, 116.3, 114.5, 110.2, 105.6, 49.3. TOF MS ES$^+$: *m/z*, $[M + Na]^+ = 258.10$.

Synthesis of platinum(II) complexes

Preparations of the platinum precursors, $Pt(COD)Cl_2$ [37], and *cis/trans*-$PtCl_2(SMe_2)_2$ [38] were carried out following the literature procedures, and their purity was confirmed by NMR, microanalysis and mass spectra.

Pt1: The complex was synthesized according to the literature procedure [39] with minor modifications. To a solution of K_2PtCl_4 (0.2 g, 0.48 mmol) dissolved in 0.005 m, HCl (100 mL) was added bis(2-pyridylmethyl)amine (0.1 mL). The solution was stirred under reflux for 3 days and then cooled to room temperature. The colourless solution was filtered and concentrated to about 10 mL. Addition of saturated $NaClO_4$ solution (2–3 mL) produced the precipitate of the desired complex. The title compound was collected by filtration and sequentially washed with small amounts of water, ethanol and ether, and dried under vacuum. Yield: 242.3 mg, yellow powder (95 %). ^{1}H NMR (DMSO-d_6, 400 MHz,): δ/ppm = 8.82 (dd, 2H), 8.60 (br s, 1H), 8.23(ddd, 2H), 7.76 (d, 2H), 7.63 (t, 2H), 4.92(m, 2H), 4.51 (dd, 2H). ^{13}C NMR (DMSO-d_6, 400 MHz): δ/ppm = 167.4, 149.4, 141.4, 125.7, 123.4, 59.4. ^{195}Pt NMR (DMSO-d_6) δ/ppm: −2,344.8. *Anal. Calcd*. for $C_{12}H_{13}N_3PtCl_2O_4$: C 27.22, H 2.46, N 7.94. *Found* C 26.72, H 2.45, N 7.62. TOF MS ES$^+$: *m/z*, $[M + H]^+ = 430.05$.

Pt2: A solution of *N*-(2-pyridylmethyl)-8-quinolinamine (0.1177 g, 0.47 mmol) in MeOH (5 mL) was added to a refluxing solution of *cis/trans*-$[PtCl_2(SMe_2)_2]$ (0.1821 g, 0.47 mmol) in MeOH (15 mL). The solution was allowed to reflux for 12 h to give an olive green residue that was collected by filtration, washed with methanol, ethanol and diethyl ether, and dried under reduced pressure. Yield: 15.1 mg, (57 %). ^{1}H NMR (DMSO-d_6, 400 MHz,): δ/ppm = 8.91 (d, 1H), 8.78(dd, 1H), 8.64 (dd, 1H), 8.54 (dd, 1H), 8.40 (td, 1H), 8.29 (ddd, 1H), 8.17–8.09 (m, 1H), 7.93 (m, 1H), 7.76 (m, 2H), 7.64 (m, 1H), 7.57 (s, 2H). ^{13}C NMR (DMSO-d_6, 400 MHz,): δ/ppm = 159.8, 148.7, 147.6, 135.7, 135.3, 128.7, 128.4, 125.0, 122.4, 121.7, 115.3, 113.5, 109.2, 106.6, 51.1. ^{195}Pt NMR (DMSO-d_6) δ/ppm: −2,514.8. *Anal. Calcd*. for $C_{15}H_{13}N_3PtCl_2$: C 35.93, H 2.59, N 8.38. *Found* C 35.44, H 2.39, N 7.91. TOF MS ES$^+$: *m/z*, $[M + H]^+ = 466.04$.

Pt3: The complex was synthesized by metal-assisted condensation of pyridine-2-carboxaldehyde and 8-aminoquinoline as proposed by Bortoluzzi et al. [40]. A suspension of *cis/trans*-$PtCl_2(SMe_2)_2$ (0.22 g, 0.57 mmol) in 20 mL of methanol was heated to 50 °C until the complete dissolution of the complex. A solution containing 8-aminoquinoline (0.082 g, 0.57 mmol) and pyridine-2-carboxyaldehyde (0.05 mL, 0.57 mmol) in 10 mL of methanol was added dropwise. The resulting solution was stirred at room temperature for 3 h. Subsequently, excess lithium perchlorate (0.35 g, 2.85 mmol) was added. A brown solid started to precipitate slowly. After maintaining the reaction mixture at −25 °C overnight, the product was filtered off, washed with methanol, ethanol and diethyl ether. Yield: 218.2 mg, (68 %). ^{1}H NMR (DMSO-d_6, 400 MHz,): δ/ppm = 9.88(s, 1H), 8.86 (dd, 1H), 8.54(d, 1H), 8.50 (dd, 1H), 8.32 (d, 1H), 8.30 (td, 1H), 8.19 (dd, 1H), 7.99 (d, 1H), 7.62 (ddd, 1H), 7.50 (t, 1H), 7.42 (d, 1H). ^{13}C NMR (DMSO-d_6, 400 MHz): δ/ppm = 166.9, 156.9, 149.0, 150.8, 149.6, 148.8, 147.5, 144.5, 141.4, 140.1, 129.6, 129.1, 126.8, 122.9, 122.1, 120.3. ^{195}Pt NMR (DMSO-d_6) δ/ppm: -2,536.3 *Anal. Calcd.* for $C_{15}H_{11}N_3PtCl_2O_4$: C 31.97, H 1.95, N 7.46. *Found* C 31.48, H1.92, N 7.91. TOF MS ES$^+$: *m/z*, $[M + H]^+ = 464.03$.

Pt4: To a reaction vessel containing BQA (132.1 mg, 0.487 mmol) and $(COD)PtCl_2$ (182 mg, 0.487 mmol)

dissolved in THF (10 mL), triethylamine (88 μL, 0.63 mmol) was added. The vessel was sealed and stirred at 95 °C for 48 h under nitrogen atmosphere. The resulting purple solution was cooled and dried in vacuo, extracted with CH_2Cl_2 (30 mL) and filtered through Celite on a sintered-glass frit. The solvent was removed under reduced pressure, and the precipitate washed with methanol (3 × 30 mL), hexane (2 × 10 mL) and diethyl ether (2 × 10 mL) and then dried in vacuo to give the desired product with spectral data consistent with those reported in a previous study [35]. Yield: 158 mg, purple powder, (65 %). ^{1}H NMR ($CDCl_3$, 400 MHz,): δ/ppm = 9.17 (d, 2H), 8.24 (d, 2H), 7.64 (d, 2H), 7.45 (t, 2H), 7.38 (m, 2H), 7.04 (d, 2H). ^{13}C NMR (CDCl3, 400 MHz,): δ/ppm = 148.9, 148.7, 148.4, 138.8, 131.4, 129.3, 121.2, 115.7, 113.4. ^{195}Pt NMR (DMSO-d_6) δ/ppm: −2,556.1 *Anal. Calcd.* for $C_{18}H_{12}N_3PtCl$: C 43.16, H 2.40, N 8.39. *Found* C 42.86, H 1.98, N 7.91. TOF MS ES$^+$: *m/z*, $[M]^+ = 500.04$.

Preparation of complex and nucleophile solutions for kinetic analysis

Platinum(II) complexes of known concentration were prepared by dissolving a specified amount in 2 % DMF to enhance the solubility and topped up with 98 % of a methanolic solvent system of 0.1 M ionic strength ($NaClO_4$). Solutions of the nucleophiles were prepared shortly before use by dissolving in a 0.1 M $NaClO_4$ solution in methanol whose ionic strength had been adjusted by addition of 10 mM LiCl to prevent any solvolysis of the complexes. The ionic strength of the solution was maintained using sodium perchlorate monohydrate ($NaClO_4$-H_2O) because the perchlorate ion (ClO_4^-) does not coordinate to Pt(II) [41, 42]. The stock solution of each nucleophile of concentration approximately 50-fold in excess of the complex was then diluted with the 0.1 M ionic strength solution to afford serial concentrations which were 40-, 30- 20- and 10-fold in excess over that of the metal complex. These concentrations of the nucleophiles were chosen to maintain *pseudo*-first-order conditions and to push the reactions to completion.

Instrumentation and measurements

^{1}H, ^{13}C and ^{195}Pt NMR spectra were recorded on a Bruker Avance III 500 or Bruker Avance III 400 spectrometer at frequencies of 500 or 400 MHz and 125 MHz/100 MHz using either a 5 mm BBOZ probe or a 5 mm TBIZ probe. All proton and carbon chemical shifts are quoted relative to the relevant solvent signal. All data were recorded at 30 °C unless stated otherwise. The mass spectrometric data of the ligands and complexes were acquired on a Waters Micromass LCT Premier spectrometer. Selected NMR and mass spectra are represented as supplementary information in Figures SI 1–15. Elemental compositions of the ligands and complexes were obtained on a Carlo Erba Elemental Analyzer 1,106. A Varian Cary 100 Bio UV–visible spectrophotometer thermostated to within ±0.05 °C was used for the kinetic measurements.

Kinetic measurements

Spectral changes resulting from mixing of the Pt(II) complex and nucleophile solutions were recorded over the wavelength range 200–650 nm to establish a suitable wavelength for kinetic measurements. The identified wavelengths are summarized in the Electronic Supplementary Information, (ESI) Table S1 1. All kinetics reactions were studied as a function of concentration and temperature under *pseudo*-first-order conditions. The kinetic data obtained were graphically analysed using the software package, Origin 7.5 [43]®. All reported rate constants represent an average value of at least three independent kinetic runs for each experimental measurement. The temperature dependence of the rate constants was studied over a range of 15–35 °C at a 5 °C interval with the nucleophile concentration being held constant at 30 times the concentration of the metal complex.

Computational modelling

Density functional theory (DFT) calculations were performed with the Gaussian 09 program suite [44] using the B3LYP method [45, 46], a three-parameter hybrid functional method, utilizing the LANL2DZ (Los Alamos National Laboratory 2 Double ζ) [47] basis set. The influence of the bulk solvent was evaluated via single-point computations using the CPCM [48, 49] formalism, i.e., B3LYP(CPCM)/LANL2DZp//B3LYP/-LANL2DZp and methanol as solvent. The complexes were each modelled at +1 or 0 with respect to their total charges.

Results

Computational analysis

In an effort to understand the interplay of structural and electronic properties of the Pt(II) complexes, DFT calculations were undertaken. As mentioned earlier, computational calculations for all the chloro platinum(II) complexes were modelled as cations except for complex Pt4 which was gauged as a neutral complex [35, 50]. The

Table 1 DFT-calculated (B3LYP(CPCM)/LANL2DZp//B3LYP/-LANL2DZp) HOMOs, LUMOs and planarity of the investigated complexes

Complex Structure	HOMO	LUMO	Planarity
 Pt1	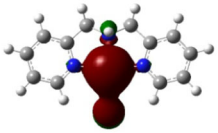	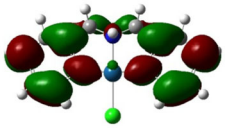	
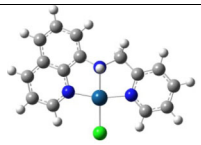 Pt2	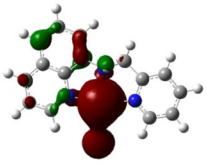	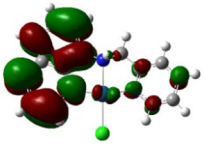	
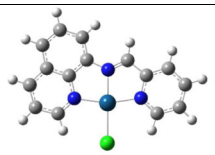 Pt3	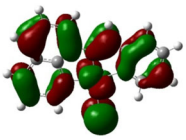	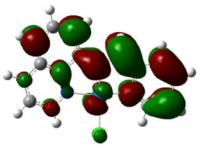	
 Pt4	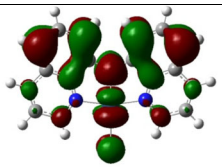	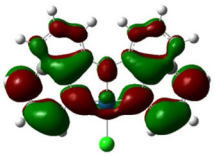	

geometry optimized structures and the mapping of the frontier molecular orbitals of the complexes are shown in Table 1. The key geometric data from DFT calculations are presented in Table 2. The HOMO–LUMO gap increases in the order of 2.890 < 3.357 < 3.571 < 3.811 for Pt4, Pt3, Pt1 and Pt2, respectively. One would expect the increase in π-conjugation would result in increase in the electrophilicity at the metal centre through π-backbonding; however; for example, in complex Pt2, the direction of the HOMO map is on the d_z^2-orbital of the metal centre signalling lack of or minimum chance of π-backbonding between the metal centre and the ligand. The LUMO in all complexes is mostly centred on the aromatic rings of the ligands with only a small contribution from the *d*-orbital on the Pt atom. The electrophilicity index (ω) (Table 2) as the measure of energy lowering due to maximal electron flow between donor and acceptor for Pt4 is found to be very small compared to other complexes, indicating that it is a poor electrophile and expected to be the least reactive complex in the series. It is evident from the optimized structures that the planarity of the complexes increases with the increase in π-conjugation.

Kinetic measurements

Substitution of labile chloride from each of the Pt(II) complexes (Scheme 1) by neutral sulphur containing

Table 2 Summary of DFT calculated parameters for complexes studied

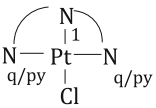	Pt1	Pt2	Pt3	Pt4
HOMO–LUMO energy				
LUMO/eV	−3.396	−2.860	−3.595	−2.284
HOMO/eV	−6.967	−6.371	−6.952	−5.174
ΔE/eV	3.571	3.511	3.357	2.890
NBO charge	0.540	0.550	0.598	0.508
Pt				
N_1	−0.637	−0.651	−0.445	−0.580
$N_{q/py}$	−0.510	−0.495	−0.494	−0.493
$N_{q/py}$	−0.510	−0.509	−0.491	−0.493
Cl	−0.497	−0,490	−0.488	−0.542
Electrophilicity index (ω)	7.518	6.067	8.284	4.811
Bond length (Å)				
Pt–N_1	2.051	2.062	1.989	2.002
Pt–$N_{q/py}$	2.040	2.037	2.037	2.029
Pt–$N_{q/py}$	2.040	2.040	2.047	2.029
Pt–Cl	2.440	2.437	2.434	2.475
Bond angles (°)				
N_1–Pt–Cl	179.43	178.35	179.41	179.91
Dipole moment (debye)	14.005	12.071	13.271	7.026

Hint: N_q and N_{py} stand for quinoline and pyridine, respectively

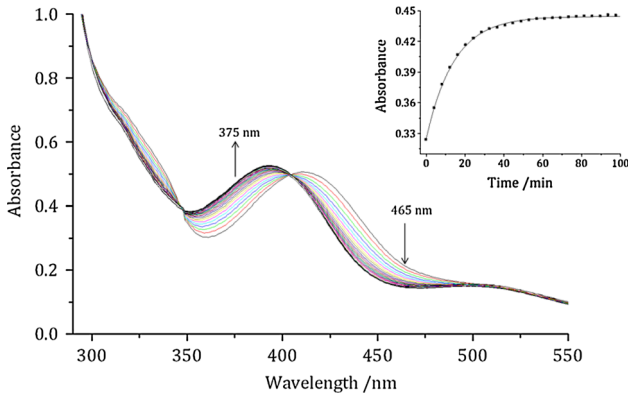

Fig. 1 UV–visible spectra recorded as a function of time for the reaction between Pt2 (0.2 mM) and TU (6 mM) at 25 °C in MeOH, $I = 0.1$ M $NaClO_4$/LiCl. *Inset* Kinetic trace obtained at 375 nm

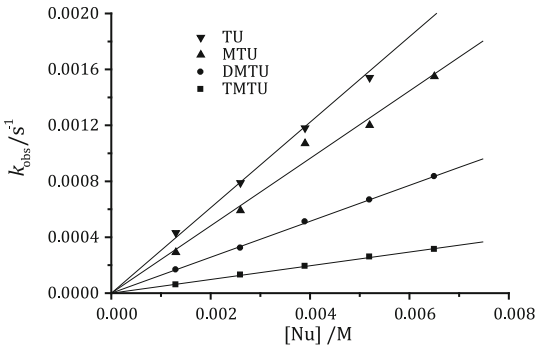

Fig. 2 Dependence of k_{obs} on the concentration of entering nucleophile for chloride substitution on Pt2 (0.20 mM) in methanol, $I = 0.1$ M ($NaClO_4$/LiCl), $T = 25$ °C

nucleophiles, namely TU, MTU, DMTU and TMTU was investigated under *pseudo*-first-order conditions and followed on a UV–visible spectrophotometer. Spectral changes resulting from mixing the complex and nucleophile (TU, MTU, DMTU and TMTU) were recorded over the 200–650 nm wavelength range, and typical representative spectra with the corresponding kinetic trace as an inset are shown in Fig. 1. The presence of certain isosbestic points in the spectra indicates a clean reaction from reactants to the product(s) [51].

All the kinetic traces for the substitution reactions gave an excellent fit to first-order exponential decay to generate observed *pseudo*-first-order rate constants (k_{obs}). These k_{obs} were plotted against the concentration of the entering nucleophile to generate the second-order rate constants, k_2 from the slopes. The plots gave straight line fits with zero intercepts as shown in the representative plots in Fig. 2 (also Figures SI 16–19) for each of nucleophiles suggesting the absence of solvolytic or parallel reactions [41]. Therefore, the rate law can be described by Eq. 1. The values of k_2 representing the direct attack of the nucleophiles on the Pt(II) metal complexes are summarized in Table 3.

$$k_{obs} = k_2[\mathrm{Nu}] \tag{1}$$

where Nu = TU, MTU, DMTU and TMTU.

The entropy of activation ($\Delta S^{\neq}$) and enthalpy of activation ($\Delta H^{\neq}$) were obtained from the Eyring plots (Fig. 3 also Figures SI 20–23) by treating the data with Eq. 2 [52] where R and T represent the gas constant and temperature, respectively.

$$\ln\left(\frac{k_2}{\mathrm{T}}\right) = \frac{-\Delta H^{\neq}}{RT} + \left(23.8 + \frac{\Delta S^{\neq}}{R}\right) \tag{2}$$

The activation data from the plots are summarized in Table 3.

Discussion

The current study focuses on understanding the competing effect of increasing π-conjugation through fusing the aromatic rings around the Pt(II) metal centre and the net σ-donor effect of the quinoline moiety which has both π-acceptor/donor phenyl as well as electron deficient pyridine ring [53, 54].

Using the substitution rate constant for coordinated chloride with TU in Pt1 as a reference, the reactivity trend follows Pt1 > Pt2 ≃ Pt3 > Pt4 with Pt1 reacting five times faster than Pt4. A similar trend in reactivity is observed for the other nucleophiles as indicated in Table 3. The observed reactivity of the investigated complexes can be accounted for in terms of the electronic effects.

The π-conjugation of the complexes in this study was varied by introducing the quinoline ligand and the imine bond. The role of extended π-conjugation on reactivity of Pt(II) complexes has been reported in the literature [1–20, 24, 27, 28]. One study showed that the reactivity of the associative substitution reaction on Pt(II) metal complexes could be increased stepwise by increasing the π-conjugation around the metal starting from Pt(dien) to Pt(terpy) [24]. Jaganyi et al. [27] have reported that extending the π-conjugation beyond the first pyridine ring surrounding the Pt(II) metal centre results in increased substitution reaction in the case of 2′-pyridyl-1,10-phenanthroline moiety but reduction in case of isoquinoline ligand moiety. The increase in reactivity due to increase in conjugation as reported in the literature [1, 2, 6–20, 24, 27, 28] is contrary to the reactivity of the complexes investigated in this study, where Pt4 which is highly conjugated is the least reactive complex in the series. This anomaly can be explained by looking at the electronic properties of the quinoline ligand which is more basic compared to pyridine as more resonance structures can be drawn to delocalize the positive charge on the conjugate acid [55]. The basic nature of the

Table 3 Summary of k_2 values and activation parameters, $\Delta H^{\neq}$ and $\Delta S^{\neq}$

Complex	Nu	$k_2 * 10^{-2}/M^{-1}\ s^{-1}$	$(\Delta H^{\neq})/kJ\ mol^{-1}$	$(\Delta S^{\neq})/J\ K^{-1}\ mol^{-1}$
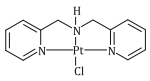 Pt1	TU	50.0 ± 0.7	50 ± 2	−130 ± 6
	MTU	43.3 ± 0.7	62 ± 4	−91 ± 15
	DMTU	16.2 ± 0.4	75 ± 3	−58 ± 10
	TMTU	3.4 ± 0.04	77 ± 1	−109 ± 4
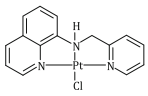 Pt2	TU	28.6 ± 0.3	59 ± 3	−104 ± 10
	MTU	24.0 ± 1.0	50 ± 2	−135 ± 6
	DMTU	12.8 ± 0.1	51 ± 1	−138 ± 3
	TMTU	4.9 ± 0.1	50 ± 2	−150 ± 5
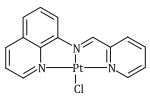 Pt3	TU	30.6 ± 0.8	48 ± 2	−141 ± 6
	MTU	28.8 ± 0.4	50 ± 1	−136 ± 4
	DMTU	14.3 ± 0.3	52 ± 2	−129 ± 7
	TMTU	5.5 ± 0.1	47 ± 2	−143 ± 7
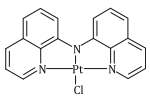 Pt4	TU	8.9 ± 0.2	53 ± 1	−129 ± 2
	MTU	8.1 ± 0.1	49 ± 1	−144 ± 5
	DMTU	4.8 ± 0.1	51 ± 1	−143 ± 3
	TMTU	2.8 ± 0.1	40 ± 2	−181 ± 7

quinoline ligands means an increase in σ-inductive effect in the complex which diminishes the π-acceptability of the ligand, in agreement with the fact that quinoline forms a number of charge transfer complexes by acting as a σ-donor [56]. The net effect of this is destabilization of the 18-electron five-coordinate transition state resulting in reduced reactivity.

In addition, according to Betley et al. [57], BQA is a typical monoanionic ligand when coordinated to a metal centre, making the resulting complexes appreciably more electron-rich than the Pt(terpy). Therefore, the weak substitution behaviour of Pt4 is due to the electron-rich environment around the metal centre and the poor π-acceptor ability of the quinoline ligand [56, 58]. This is supported by the DFT calculations, which show the electrophilicity index of the complexes as a whole decreases from Pt1 to Pt4 with the exception of Pt3. This is because the introduction of the imine bond in Pt3 changes the nature of the *trans*-effect and accounts for its DFT values falling out of the line with those of the other complexes. The DFT calculations also show that the Pt–N_q bond length is shorter in Pt4 compared to the other complexes, an indication of stronger σ-interaction between the Pt metal and the *cis* nitrogen atom. This is supported by the NBO charges, which show Pt4 to be less positive than the rest.

The increase in π-conjugation is reflected in the HOMO–LUMO energy gap which decreases from Pt1 to Pt4 indicating that the complexes become softer and as such should be more reactive [59, 60]. This is counteracted by the electrophilicity and the dipole moment of the complexes which are in agreement with the reactivity trend. It can therefore be concluded that the electron-rich environment around the ligand moiety is responsible for decreasing the electrophilicity of the complexes as observed. This in turn retards the entry of the incoming nucleophiles through repulsion, slowing the rate of substitution of the chloride ligand. It is clear that π-backbonding in these systems is weaker than the dominant σ-donation from the quinoline moiety.

From the DFT calculations, the π^*-orbitals of the BQA ligand are of appropriate symmetry to mix with a filled metal $d\pi$-orbital; however, the LUMO energies in Pt4 (−2.284 eV) are very high (Table 2) in relation to Pt1 (−3.396 eV), Pt2(−2.860 eV) and Pt3(−3.595 eV). The rise in the LUMO energy describes Pt4 as a hard/poor electrophile [59, 60] and this is expected to result in dampening the general reactivity. The increase in the LUMO energy levels with expansion of the π-system observed for Pt4 and Pt2 is attributed to the either increase in total antibonding character or an increased localization of the π^*-orbital on the complexes [61–63].

What is observed is that introducing an imine bond in Pt3 results in a slight increase in the reactivity of Pt3 compared to Pt2. This is mostly due to the increase in π-communication which increases the π-backbonding of the Pt(II) metal centre and the change in the *trans*-effect [19, 20, 64]. The fact that the reactivity hardly changes moving from Pt2 to Pt3 is in support that the net σ-effect around the ligand moiety is stronger and controls the reactivity of these complexes. What is also noted from the DFT

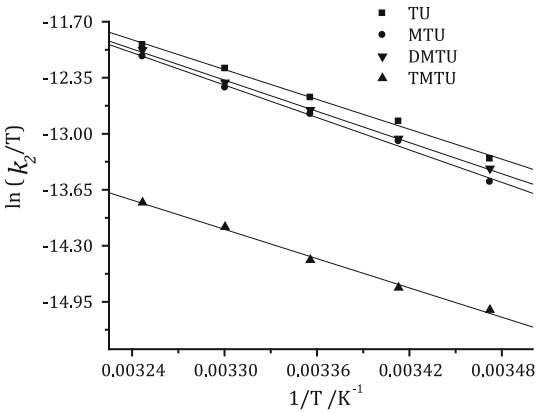

Fig. 3 Eyring plots for the reaction of Pt3 with a series of neutral nucleophiles at various temperatures in range of 15–35 °C

calculations is that introduction of quinoline increases the planarity of the complexes from Pt1 to Pt4. However, even though this has significant effect on the π-backbonding, it had little or no effect in influencing the reactivity trend of the complexes investigated. In all Pt(II) complexes investigated, the trend in dipole moment is in accord with the reactivity of the complexes given that the parameter correlates with the π-withdrawing character of the complex [65]. Pt1 contains two π-acceptor pyridine rings in *cis* position relative to the leaving ligand. The π-acceptor ligands withdraw electron density from the Pt(II) centre, making it more electrophilic for a nucleophilic attack and stabilization of the electron-rich five-coordinate transition state. This results in a reduction in the activation barrier and an acceleration of the reaction observed for Pt1.

The reactivity of the nucleophiles follows the trend TU > MTU > DMTU > TMTU for all complexes which is in agreement with the steric hindrance and their sizes. The large negative values of entropy, $\Delta S^{\#}$, and positive enthalpy, $\Delta H^{\#}$, of activation support an associative mechanism that is typical of Pt(II) square planar complexes [66–69].

Conclusion

This study has shown that tuning electronic communication at Pt(II) metal centres towards ligand substitution reactions using quinoline-based ligands has an opposite effect to that reported for pyridine ligands. It is evident that increasing electronic communication without increasing π-backbonding has little effect in increasing the reactivity of a Pt(II) complex. In Pt4, the electronic communication based on the number of aromatic rings connected together is greater than for the Pt-terpy system, but the rate of reaction is 10^5 slower. This is because of the σ-inductive effect of the quinoline ligands towards the metal centre which weakens the π-backbonding effect of the aromatic system. This effect is very dominant and controls the reactivity of the metal complex, which remains associative in nature.

Electronic supplementary information (ESI)

The available ESI includes a number of NMR and mass spectra, wavelengths for kinetic measurements, concentration dependence and Eyring plots for determination of second-order rate constant and activation parameters, respectively, planarity and electrostatic potential map of the investigated complexes.

Acknowledgments The authors thank the University of Dar es Salaam (Tanzania) and University of KwaZulu-Natal (South Africa) for financial support to Grace Kinunda.

References

1. Jaganyi D, Reddy D, Gertenbach JA, Hoffman A, van Eldik R (2004) J Chem Soc Dalton Trans (2):299
2. Ertürk H, Puchta R, van Eldik R (2009) Eur J Inorg Chem (10):1331
3. Deubel V (2002) J Am Chem Soc 124:5834
4. Lemma K, Elm Roth SKC, Elding LI (2002) J Chem Soc Dalton Trans (7):1281
5. Teuben J, Rodriguez M, Zubiri I, Reedijk J (2000) J Chem Soc Dalton Trans (3):369
6. Jaganyi D, Tiba F (2003) Transit Met Chem 28:803
7. Jaganyi D, Tiba F, Munro OQ, Petrović B, Bugarčić ŽD (2006) J Chem Soc Dalton Trans (24):2943
8. Bugarčić ŽD, Liehr G, van Eldik R (2002) J Chem Soc Dalton Trans (6):951
9. Pitteri B, Annibale G, Marangoni G, Cattalini L, Visentin F, Bertilasi V, Gilli P (2001) Polyhedron 20:869
10. Annibale G, Brandolisio M, Pitteri B (1995) Polyhedron 14:451
11. Bogojeski J, Bugarčić ŽD (2011) Transit Met Chem 36:73
12. Annibale G, Brandolisio M, Bugarčić ŽD, Cattalini L (1998) Transit Met Chem 23:715
13. Pitteri B, Marangoni G, Cattalini L, Viseulim FV, Bobbo T (1998) Polyhedron 17:475
14. Petrović B, Djuran MI, Bugarčić ŽD (1999) Met Based Drugs 6:355
15. Pitteri B, Annibale G, Marangoni G, Bertilasi V, Ferretti V (2002) Polyhedron 21:2283
16. Bugarčić ŽD, Heinmann FW, van Eldik R (2004) J Chem Soc Dalton Trans (2):279
17. Reddy D, Jaganyi D (2008) Dalton Trans (47):6724
18. Jaganyi D, de Boer K, Gertenbach J, Perils J (2008) Int J Chem Kinet 40(12):808
19. Petrović B, Bugarčić ŽD, Dees A, Ivanović-Burmazović I, Puchta R, Heinemann FW, Steinmann SN, Corminboeuf C, van Eldik R (2012) Inorg Chem 51:1516
20. Đurović M, Bogojeski J, Petrović B, Petrović D, Heinemann FW, Bugarčić ŽD (2012) Polyhedron 41:70
21. Williams JAG (2009) Chem Soc Rev 38:1783
22. Burdett JK (1975) Inorg Chem 14:931

23. Burdett JK (1977) Inorg Chem 16:3013
24. Jaganyi D, Hofmann A, van Eldik R (2001) Angew Chem Int Ed 40:1680
25. Hofmann A, van Eldik R (2003) Dalton Trans (15):2979
26. Mambanda A, Jaganyi D (2011) Dalton Trans 40:79
27. Ongoma P, Jaganyi D (2012) Dalton Trans 41:10724
28. Reddy D, Akerman KJ, Akerman MP, Jaganyi D (2011) Transit Met Chem 36:593
29. Rosenberg B, Van Champ L, Trosko JE, Mansour VH (1969) Nature 22:385
30. Florea A-M, Büsselberg D (2011) Cancers 3:1351
31. Dempke W, Voigt W, Grothey A, Hill BT, Schmoll HJ (2000) Anticancer Drugs 11:225
32. Wang J, Wang X, Song Y, Zhu C, Wang J, Wang K, Guo Z (2013) Chem Commun 49:2786
33. Pabla N, Dong Z (2012) Oncotarget 3(1):107
34. Carlsen L, Egsgaard H, Anderson JR (1979) Anal Chem 51:1593
35. Peters JC, Harkins SB, Brown SD, Day MW (2001) Inorg Chem 40:5083
36. Incarvito C, Lam M, Rhatigan B, Rheingold AL, Qin CJ, Gavrilova AL, Bosnich B (2001) J Chem Soc Dalton Trans (23):3478
37. Clark HC, Manzer LE (1973) J Organomet Chem 59:411
38. Darensbourg MY, Hill GS, Irwin MJ, Levy CJ, Rendina LM, Puddephatt RJ, Andersen RA, Mclean L (2007) Inorg Synth 32:149
39. Weber CF, van Eldik R (2005) Eur J Inorg Chem (23):4755
40. Bortoluzzi M, Paolucci G, Pitteri B, Zennaro P, Bertolasi V (2011) J Organomet Chem 696:2565
41. Hofmann A, Dahlenburg L, van Eldik R (2003) Inorg Chem 42:6528
42. Appleton TG, Hall JR, Ralph SF, Thompson CM (1984) Inorg Chem 41:3521
43. Origin7.5®™ SRO, v7.5714 (B5714), Origin Lab Corporation, Northampton, One, Northampton, MA, 01060, USA, 2003
44. Frisch MJ, Trucks GW, Schlegel HB, Scuseria GE, Robb MA, Cheeseman JR, Scalmani G, Barone V, Mennucci B, Petersson GA, Nakatsuji H, Caricato M, Li X, Hratchian HP, Izmaylov AF, Bloino J, Zheng G, Sonnenberg JL, Hada M, Ehara M, Toyota K, Fukuda R, Hasegawa J, Ishida M, Nakajima T, Honda Y, Kitao O, Nakai H, Vreven T, Montgomery JA Jr., Peralta JE, Ogliaro F, Bearpark M, Heyd JJ, Brothers E, Kudin KN, Staroverov VN, Kobayashi R, Normand J, Raghavachari K, Rendell A, Burant JC, Iyengar SS, Tomasi J, Cossi M, Rega N, Millam JM, Klene M, Knox JE, Cross JB, Bakken V, Adamo C, Jaramillo J, Gomperts R, Stratmann RE, Yazyev O, Austin AJ, Cammi R, Pomelli C, Ochterski JW, Martin RL, Morokuma K, Zakrzewski VG, Voth GA, Salvador P, Dannenberg JJ, Dapprich S, Daniels AD, Farkas O, Foresman JB, Ortiz JV, Cioslowski J, Fox DJ (2009) Revision A.1 Gaussian, Inc., Wallingford, CT. http://akira.ruc.dk/~spanget/help/g09/m_citation.htm
45. Becke AD (1993) J Chem Phys 98:5648
46. Lee CT, Parr RG (1988) Phys Rev B 37:785
47. Hay PJ, Wadt WR (1985) J Chem Phys 82:299
48. Barone V, Cossi M (1998) J Phys Chem A 102:1995
49. Cossi M, Scalmani G, Rega N, Barone V (2003) J Comput Chem 24:669
50. Harkins SB, Peters JC (2002) Organometallics 21:1753
51. Ray M, Bhattacharya S, Banerjee P (1999) Polyhedron 18:1569
52. Eyring H (1935) J. Chem. Phys. 3:107
53. http://myweb.unomaha.edu/~dstack/2250/Overheads/EWG_EDG.PDF. Accessed 15th Mar 2013
54. Bruice PY (1998) Organic chemistry, 2nd edn. Prentice-Hall Inc, New Jersey
55. Hosmane RS, Liebman JF (2009) Struct Chem 20:693
56. Gurnos J (2009) *The Chemistry of heterocyclic compounds*. In: Quinolines, vol 32. Wiley, London, p 9
57. Betley TA, Qian BA, Peters JC (2008) Inorg Chem 47:11570
58. Suzuki T, Kuchiyama T, Kishi S, Kaizaki S, Takagi HD, Kato M (2003) Inorg Chem 42(3):785
59. Singh RK, Verma SK, Sharma PD (2011) Int J Chem Tech Res 3(3):1571
60. Chattaraj PK, Maiti B (2003) J Am Chem Soc 125:2705
61. Adachi M, Nagao Y (2001) Chem Mater 13:662
62. Adachi M, Murata Y (1998) J Phys Chem A 102:841
63. Juris A, Barigelletti F, Balzani V, Belser P, von Zelewsky A (1985) Inorg Chem 24:202
64. Romeo R, Plutino MR, Scolaro LM, Stoccoro S, Minghetti G (2000) Inorg Chem 39:4749
65. Rillema DP, Cruz AJ, Moore C, Siam K, Jehan A, Base D, Nguyen T, Huang W (2013) Inorg Chem 52:596
66. Basolo F, Pearson RG (1967) Mechanisms of inorganic reactions, 2nd edn. Wiley, New York, pp 80–115
67. Purcell KF, Kotz I (1977) Inorganic chemistry. Holt-Saunders, Philadelphia, pp 694–755
68. Tobe ML, Burgess J (1999) Inorganic reaction mechanisms. Addison Wisey, Longman, Ltd., Essex, pp 30–33, 70–112
69. Atwood JD (1997) Inorganic and organometallic reaction mechanisms, 2nd edn. Wiley-VCH Inc, New York, pp 43–61